Fish distribution in three dimensions around the Block Island Wind Farm as observed with conventional and volumetric echosounders

J. Michael Jech[1] | **Andrew Lipsky[1]** | **Patrick Moran[2]** | **Guillaume Matte[3]** | **Gabriel Diaz[4]**

[1]National Oceanic and Atmospheric Administration, Northeast Fisheries Science Center, Woods Hole, Massachusetts, USA

[2]iXblue, Denver, Colorado, USA

[3]iXblue Sonar Division, La Ciotat, France

[4]IBSS, Miami, Florida, USA

Correspondence
J. Michael Jech
Email: michael.jech@noaa.gov

Abstract

Objective: Offshore wind development is expected to expand rapidly along the East Coast of the United States within the next 10 years and will impact the biology and ecology of the flora and fauna as well as human activities, such as commercial and recreational fishing. The Block Island Wind Farm is a five-turbine, 30-MW wind array located about 6 km off the coast of Rhode Island and has been in operation since 2016.

Methods: We conducted a 4-day acoustical and biological survey of the area during daylight hours to gain insight on the spatial distribution of fish species in and around the turbines. We utilized a hull-mounted, downward-looking Simrad 38-/200-kHz ES70 and a pole-mounted iXblue SeapiX steerable Mills Cross, 150-kHz, 1.6° resolution multibeam echosounder oriented downward to map the two- and three-dimensional distributions using spiral and straight-line transect patterns. We collected fish by using hook and line to verify the sources of acoustic backscatter and to measure length, sex, and diet.

Result: Black Sea Bass *Centropristis striata* were the most commonly caught species and appeared to be the primary constituents of the fish aggregations that were mapped by the acoustic systems. We found increased levels of acoustic backscatter within 200 m of the turbine structures, suggesting that they were attractive structures.

Conclusion: These levels were not greater than backscatter levels in the surrounding area, suggesting that the proximate effect of the wind array was spatially limited.

KEYWORDS
acoustics, multibeam, offshore wind, survey methods

INTRODUCTION

Offshore wind development will be a large part of the seascape along the Atlantic coast of the United States. There are 930,777 ha (2.3 million acres) of continental shelf leases proposed for offshore wind development by 2030, producing nearly 30 GW of electricity (Bureau of Ocean Energy Management 2022). Another 7.3 million ha (18 million acres) are currently under the Bureau of Ocean Energy Management's planning phase for designation of future offshore wind development areas (OWDAs) beyond 2030 (Bureau of Ocean Energy Management 2023). These areas will have local and regional ecological and socioeconomic effects that have yet to be fully characterized (Methratta and Dardick 2019). Structures, whether they are natural (e.g., rocky reefs or coral reefs) or artificial (e.g., oil and gas platforms, submerged wrecks, or wind turbines), provide additional substrate and protection that allow marine flora and fauna to flourish (Bohnsack and Sutherland 1985; Bull and Love 2019). These structures can attract smaller prey species, which in turn attract larger predators (Becker et al. 2023), resulting in higher biomass and potentially increased production (Claisse et al. 2014) in and near these structures.

The potential effects of OWDAs on finfish and shellfish populations are a major issue for federal and local governments that manage fisheries resources. Offshore wind development areas can have proximate effects whereby abundance and biomass are enhanced at or near turbines (Stanley and Wilson 1997; Paxton et al. 2019), and these effects may or may not "spill over" to the greater population and increase production (Bohnsack 1989; Claisse et al. 2014; Smith et al. 2016; Roa-Ureta et al. 2019; Schwartzbach et al. 2020). Hence, it is important to understand the extent to which these OWDAs may affect fisheries resources, surveys, and commerce (Gill et al. 2020). The National Oceanic and Atmospheric Administration's (NOAA) Northeast Fisheries Science Center (NEFSC) has been conducting finfish surveys since the 1960s using bottom trawls deployed from NOAA fisheries research vessels (Azarovitz 1981; Politis et al. 2014) and has been conducting shellfish dredge surveys since the late 1970s (e.g., Clark et al. 1999; Miller et al. 2019; O'Keefe 2022). These surveys cover large portions of the U.S. continental shelf from Cape Hatteras, North Carolina, north to Canadian waters in the Gulf of Maine, with multiple surveys throughout the year, and data from these surveys can be critical for population assessments. For example, the NEFSC bottom trawl survey provides data for population assessments of 35 species, with 21 species' assessments being completely or heavily reliant on

Impact statement

Black Sea Bass were found in enhanced numbers at the Block Island Wind Farm, suggesting that it provides habitat for Black Sea Bass and other fish species that are attracted to reefs and other structures.

those data (NEFSC, unpublished data). Due to a variety of factors (such as navigational safety concerns and maneuverability while deploying scientific gear and instruments), most of these NOAA surveys likely will not be able to traverse or sample in OWDAs, so the NEFSC has initiated efforts to evaluate the impact of OWDAs on stock assessments as well as to develop alternative methods, such as optical (e.g., Miller et al. 2019) and acoustical technologies (e.g., Jech and Sullivan 2014; Jech and McQuinn 2016), to collect the necessary data for stock assessments (Hare et al. 2022).

Although several OWDAs are currently scheduled for development, at present there are only two OWDAs with active turbines in U.S. state waters and/or the U.S. exclusive economic zone: the Block Island Wind Farm (BIWF) and the Coastal Virginia Offshore Wind Area. The BIWF is situated off the coast of Rhode Island (Figure 1) and has been in operation since 2016, nominally providing 30 MW of electricity. It consists of five wind turbine generators (WTG-1–5, with WTG-1 at the northeast end and WTG-5 at the southwest end) that are affixed to the seabed (Wilber et al. 2022a) in 20–30 m of water. Each of the five WTGs is supported by a 15.24-×15.24-m, four-leg jacket foundation that is secured to the seafloor with four through-the-leg foundation piles that are between 106.7 and 137.2 cm in diameter, and the pin piles are driven to a depth of up to 76.2 m (HDR 2018). The individual four-leg jacket foundations consist of aluminum anodes and steel lattice framing composed of 76.2–91.4-cm-diameter rods, and each of the four jacket legs is 1.52–1.70 m in diameter (S. Wilkey, Ørsted North America, personal communication). Ideally, resource surveys in and near OWDAs are conducted before, during, and after construction of the wind turbines (e.g., before–after, control–impact [BACI] design; Methratta 2020, 2021). In the case of the BIWF, Wilber et al. (2022b) showed species-specific responses to construction and operation phases using monthly trawl surveys and a BACI survey design.

Over the course of 4 days, we conducted multiple acoustical surveys with biological sampling in and around the BIWF. We followed a distance-based, after-gradient method (Methratta 2021) wherein we
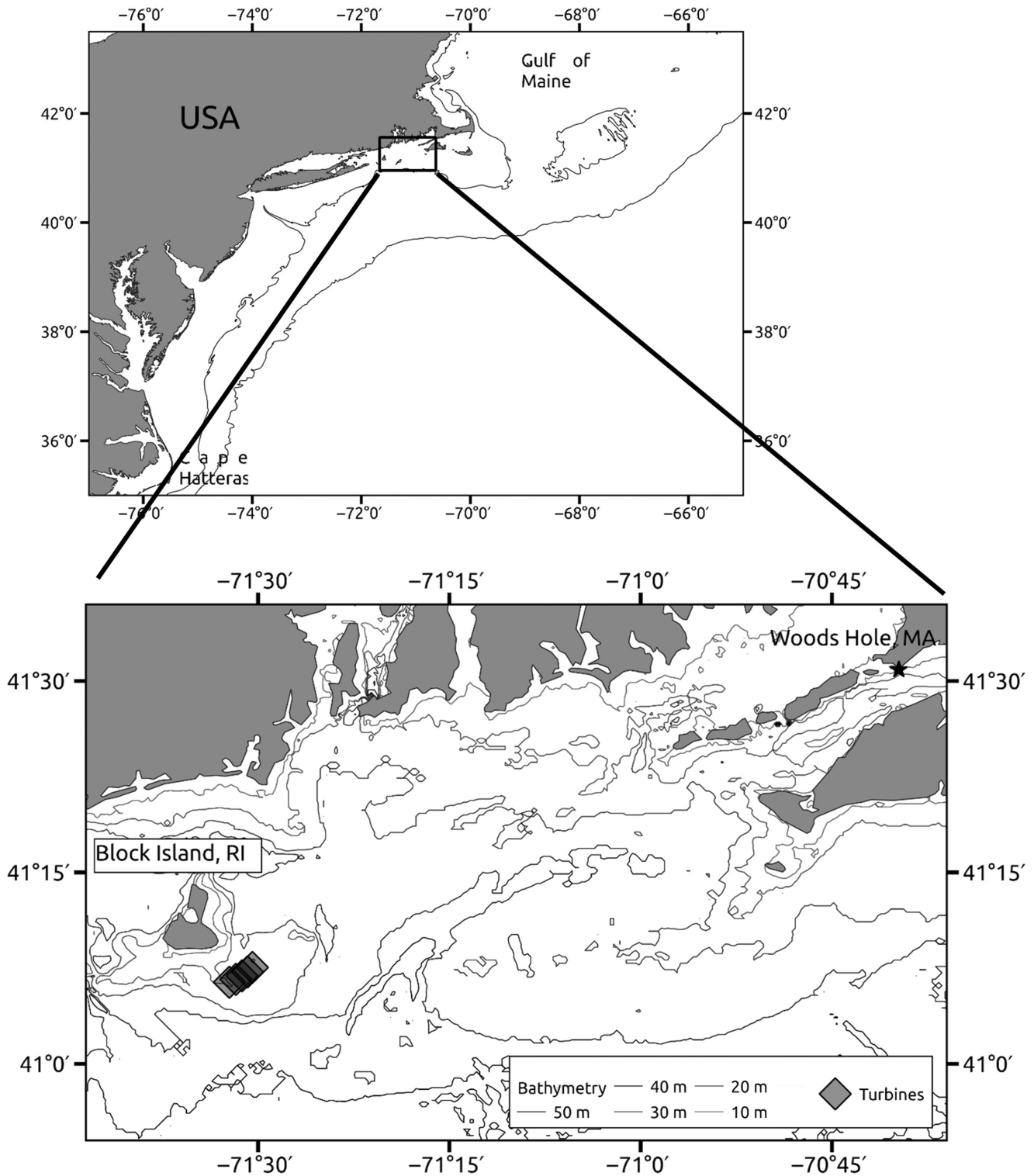
FIGURE 1 Location of the Block Island Wind Farm (turbine locations, lower panel) along the East Coast of the United States.

surveyed at varying distances from each turbine as well as the collection of turbines (i.e., the wind array). Our goal was to investigate the influence of turbine structures on finfish distribution by mapping the spatial distribution of pelagic animals within and away from the proximity of the turbines using active acoustic methods and collection of biological samples. We believe this to be the first systematic study of the BIWF using active acoustical methods with single-beam and multibeam echosounders, and we hoped to gain insights into the distribution of pelagic species in and around the BIWF and to assess alternative sampling technologies and

survey modalities that can be used in future OWDAs along the U.S. coast.

METHODS

Survey design

Acoustic and biological data were collected primarily during daylight hours on August 10–13, 2021, from the RV *Gloria Michelle*. Acoustic data were collected with single-beam and multibeam echosounders, and fish specimens were collected by hook and line. August 10 and 13 were transit days to/from Woods Hole, Massachusetts, and to/from the BIWF as well as surveys of the BIWF. We conducted five survey patterns in and near the BIWF (Figure 2): (1) transects parallel to the northeast–southwest (NE–SW) axis of the turbines to examine distributions at and between turbines; (2) transects in a north–south direction alongside each turbine; (3) parallel transects orthogonal to the NE–SW axis of the BIWF, with the transects bisecting the distance between each turbine; (4) spiral patterns that began within 30–50 m of each turbine and spiraled outward at approximately 50–60-m spacing until the final spiral was completed approximately halfway between the turbine being surveyed and the next turbine; and (5) ad hoc transects that surveyed the aggregations of fish observed to the south and west of WTG-5. We attempted to get as close to the turbines as the vessel command was comfortable with while minimizing the ensonification of the turbine structure with the 38-kHz acoustic beam.

Biological data

We focused our biological sampling effort on finfish. Specimens were collected on an ad hoc basis using hook-and-line angling with standard light spin tackle with 22.7-kg-test (50-lb-test) braided line and 22.7-kg-test monofilament leader. Metal lures (142–198 g [5–7 oz]) were jigged at depths where the echosounders observed fish and were cast and retrieved near the surface. Angling is an effective method for sampling fish when other capture methods, such as trawls, are not available (e.g., Frear 2002; Fernandes et al. 2016; Dainys et al. 2022). Some specimens were caught and released with no measurements (i.e., catch and release), some were caught and only their lengths were measured, and others were measured and dissected to examine sex, maturity stage, and stomach contents using procedures consistent with NEFSC bottom trawl survey protocols (Politis et al. 2014). Specimens that were brought on board were identified to

species, and fish that were hooked but not landed were identified only if we were able to do so visually. Length measurements were either fork length or total length, depending on the species.

Dual-frequency, single-beam data

A Simrad ES70 echosounder transmitted 0.512-ms pulses at a transmit rate of 2 Hz (0.5-s interval) simultaneously at 38 and 200 kHz with a hull-mounted Simrad 38-/200-kHz Combi-C transducer. The 38-kHz beam pattern was elliptical, with 21° transverse and 13° longitudinal beam widths (measured at the half-power points); the 200-kHz beam pattern was circular, with a 7° beam width. The ES70 was calibrated using a 38.1-mm-diameter tungsten carbide sphere with 6% cobalt binder on August 16, 2021, as per standard procedures (Foote et al. 1987). Data were collected continuously throughout the survey and recorded to a portable hard drive. Data were processed, analyzed, and visualized using Echoview version 12 (www.echoview.com), Python version 3+, R statistical software (R Core Team 2022), and QGIS version 3.20 (QGIS 2022).

Data from the top 3 m were removed from analysis to eliminate the transmit pulse and surface bubbles. Additional water depth was excluded when surface bubbles extended deeper than 3 m using Echoview's "Bad Data (no data)" classification and visual scrutiny. The seabed echo was detected using Echoview's "best bottom candidate" algorithm with a 0.5-m backstep, and the resulting line was visually inspected and manually corrected if necessary. Data deeper than the seabed detected line were excluded from all analyses. An impulse noise filter (Ryan et al. 2015) was applied to the data using a vertical and horizontal window of five range/depth samples and five pings, respectively, to remove cross talk among different acoustical systems on board. We set the equivalent distance sampling unit (EDSU) to 40 m based on the acoustic beam diameters at 50-m range of 18.5 m for the 21° 38-kHz beam and 6.1 m for the 7° 200-kHz beam. The choice of 40 m for EDSU size also set the minimum distance to the turbines because we wanted to minimize the probability of ensonifying part of the turbine structure and artificially inflating backscatter within EDSUs that were close to the turbines. A minimum volume backscatter (S_v; dB referenced to [re] $m^2\,m^{-3}$) threshold of -80 dB was applied to the data. The 38- and 200-kHz areal backscatter (S_a; dB re $m^2\,m^{-2}$) values were computed for each 40-m EDSU ($S_{a,\mathrm{EDSU}}$[38 kHz] and $S_{a,\mathrm{EDSU}}$[200 kHz]) throughout the water column (between the surface exclusion zone and 0.5 m above the seabed echo).
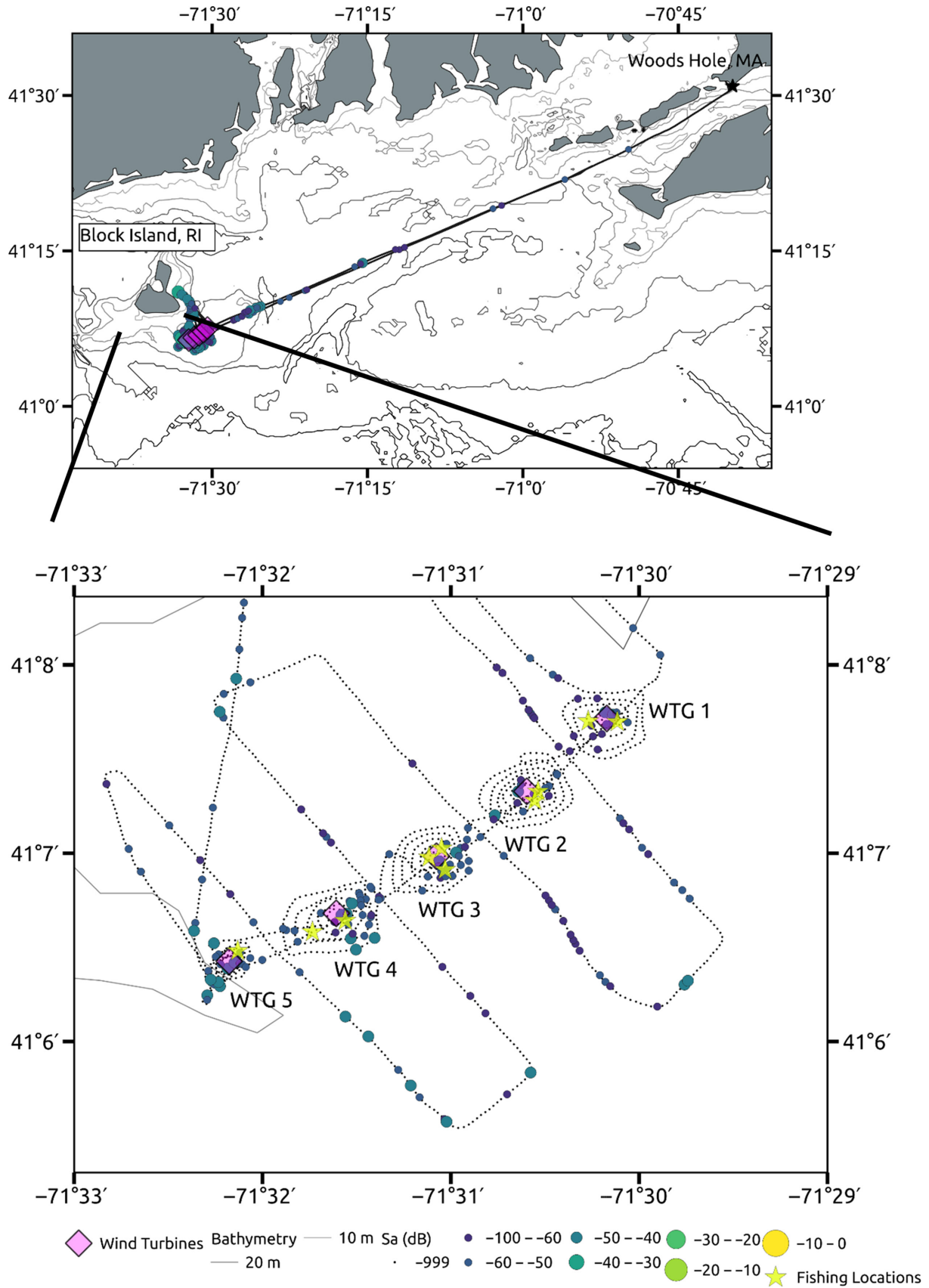
FIGURE 2 Cruise tracks for August 10–13, 2021 (top panel), and August 11, 2021 (lower panel). Spiral and parallel transect patterns were conducted on August 11. The S_a (dB referenced to 1 m² m⁻²) values represent acoustic backscatter for regions at 38 kHz. The yellow stars represent the approximate angling locations.

A decibel differencing method was used to assist with separating backscatter from animals with a gas inclusion (e.g., fish with a gas-filled swim bladder) from those without (Kang et al. 2002; Korneliussen 2018). We subtracted the S_v (dB re 1 m^2 m^{-3}) at 38 kHz from the S_v at 200 kHz for each acoustic bin ($\Delta S_v = S_v[200$ kHz$] - S_v[38$ kHz$]$), where each bin was one ping by one range/depth sample (0.1 m). Values of ΔS_v between -4 and -40 dB were considered to represent fish with a gas-filled swim bladder. These bins were used to classify backscatter to a generic "fish" category. Final classification was done visually and polygon regions were drawn manually on echograms, circumscribing backscatter that was classified as "fish." The final classification regions were applied to the 38- and 200-kHz S_v data. The S_a and geographic location of the region midpoint, as well as vertical distribution metrics of center of mass, inertia, proportion occupied, equivalent area, and aggregation index (Urmy et al. 2012) for each region ($S_{a,\text{region}}[38$ kHz$]$), were used to map the spatial distributions of fish in and around the BIWF. Acoustic data from all survey designs and tracks were used in the analyses for which we pooled all echosounder data and did not make comparisons among survey designs.

Spatial proximity to wind turbines

To address whether the wind array and/or individual turbines affected the spatial distribution of fish, we examined the measures of fish abundance (using S_a as a proxy), location (midpoints of each EDSU or region), and vertical distribution (Urmy et al. 2012) as a function of distance to the BIWF geographic midpoint and to each turbine. We used the geographic midpoint of all turbines as representative of the BIWF, and we used the geographic location of each turbine as representative of the individual turbines. Distances between the midpoints of each EDSU or region and the BIWF midpoint or each turbine were computed using the R package geodist (https://github.com/hypertidy/geodist). Latitudes and longitudes of the turbines were obtained from an ArcGIS File Geodatabase (Northeast Ocean Data; www.northeastoceandata.org). The geographic midpoint of the turbines was calculated by averaging the latitudes and longitudes separately, and we assumed that the curvature of the Earth had minimal impact over the approximately 3.5-km extent of the BIWF. The EDSU and region geographic midpoints were generated by Echoview. For each EDSU and region, the closest turbine was selected (i.e., the minimum distance between each EDSU or region and each turbine) as the "closest point of approach" (CPA) to the turbines.

Multibeam data

Multibeam data were collected with an iXblue SeapiX multibeam echosounder sonar. SeapiX is a three-dimensional volumetric multibeam echosounder composed of a dual steerable Mills Cross sonar transducer. The two transducer arrays are centered on one another, allowing for full 120° swaths to be steered in either the along-track or across-track orientation. Beam width varies from 1.6° for the central beams to 3.2° for the outer beams, and the beams are stabilized on transmission using real-time motion data from an internal micro-electromechanical system inertial measurement unit. The use of bidirectional arrays capable of both transmission and reception allows for split-beam processing of the data. A source level of 214 dB was applied for this survey.

The model used for the survey was a SeapiX Light, which consisted of a positively buoyant, 27-kg sonar head; cabling; and a ruggedized case. The sonar head housed the transducers as well as their power electronics and signal digitization electronics; it was pole mounted at the port aft of the RV *Gloria Michelle*, 1 m below the water line, and was oriented either downward or sideways (with a 10° tilt) looking. The case was strapped down below deck and housed the processing unit as well as the 36-V input power supply for the whole system. A 20-m deck cable (2 cm in diameter) connected the topside unit to the sonar head, provided an Ethernet connection for data flow, and supplied power to the transducer electronics, while a laptop was used for data collection and monitoring. A 1-ms-duration, linear frequency modulation pulse with a center frequency of 150 kHz and a 10-kHz bandwidth was transmitted at a rate of 8–10 Hz.

Multibeam SeapiX data were converted by iXblue to a format that could be read and processed in Echoview version 12+ using custom-built MATLAB code from iXblue. Individual targets within the swath were detected in Echoview using the "unspecified decibel" data. A three-dimensional convolution was applied using Echoview's "XxYxZ operator" to calculate the mean value within a window size of 3 range samples × 3 beams × 3 pings. Single targets were detected in the entire swath using Echoview's "multibeam target detection 1" algorithm with the default settings. A target conversion was applied to calculate the true geographical position and depth for each single target, and single-target information was exported to a text file. Echo strength (dB re m^2) for each individual target was generated by iXblue and exported to a text file. Single-target data were visualized in QGIS and analyzed in RStudio.

RESULTS

Hook-and-line sampling

One Little Skate *Leucoraja erinacea*, one Scup *Stenotomus chrysops*, four Bluefish *Pomatomus saltatrix*, and 22 Black Sea Bass *Centropristis striata* were caught during the cruise period (Table S1). Black Sea Bass lengths ranged from 22 to 47 cm; the larger individuals were male, and the smaller individuals were female. All but one of the Black Sea Bass were in developing condition (five individuals) or spawning condition (two ripe individuals and three ripe and running individuals). Stomach contents consisted of unidentified crabs, Northern Sand Lance *Ammodytes dubius*, and longfin inshore squid *Doryteuthis pealeii*. We did not record catch time to the precision necessary for precise geolocation of catches, but we did record the approximate times for a qualitative view (Figure 2).

Dual-frequency, single-beam acoustic data

Due to the disparity in beam widths between the 38- and 200-kHz acoustic beams (21°×13° [38 kHz] vs. 7° [200 kHz]), the decibel differencing method provided only visual assistance with selecting backscatter that was attributed to fish (Figure 3). The final classification of backscatter to the generic category "fish," which represented fish with gas-filled swim bladders, was done manually by drawing polygons around areas (i.e., regions) of the 38-kHz echogram. Backscatter within these polygons was analyzed as fish regions. Backscatter within and outside of these regions was analyzed as total backscatter (i.e., total backscatter included fish backscatter).

Dual-frequency, single-beam acoustic data spanned nearly a 90-km range (including transits), with most data collected within about 10 km of the BIWF (Figures 2 and 4). An overall increase in $S_{a,EDSU}$ from Woods Hole (right side of each panel in Figure 5) to about

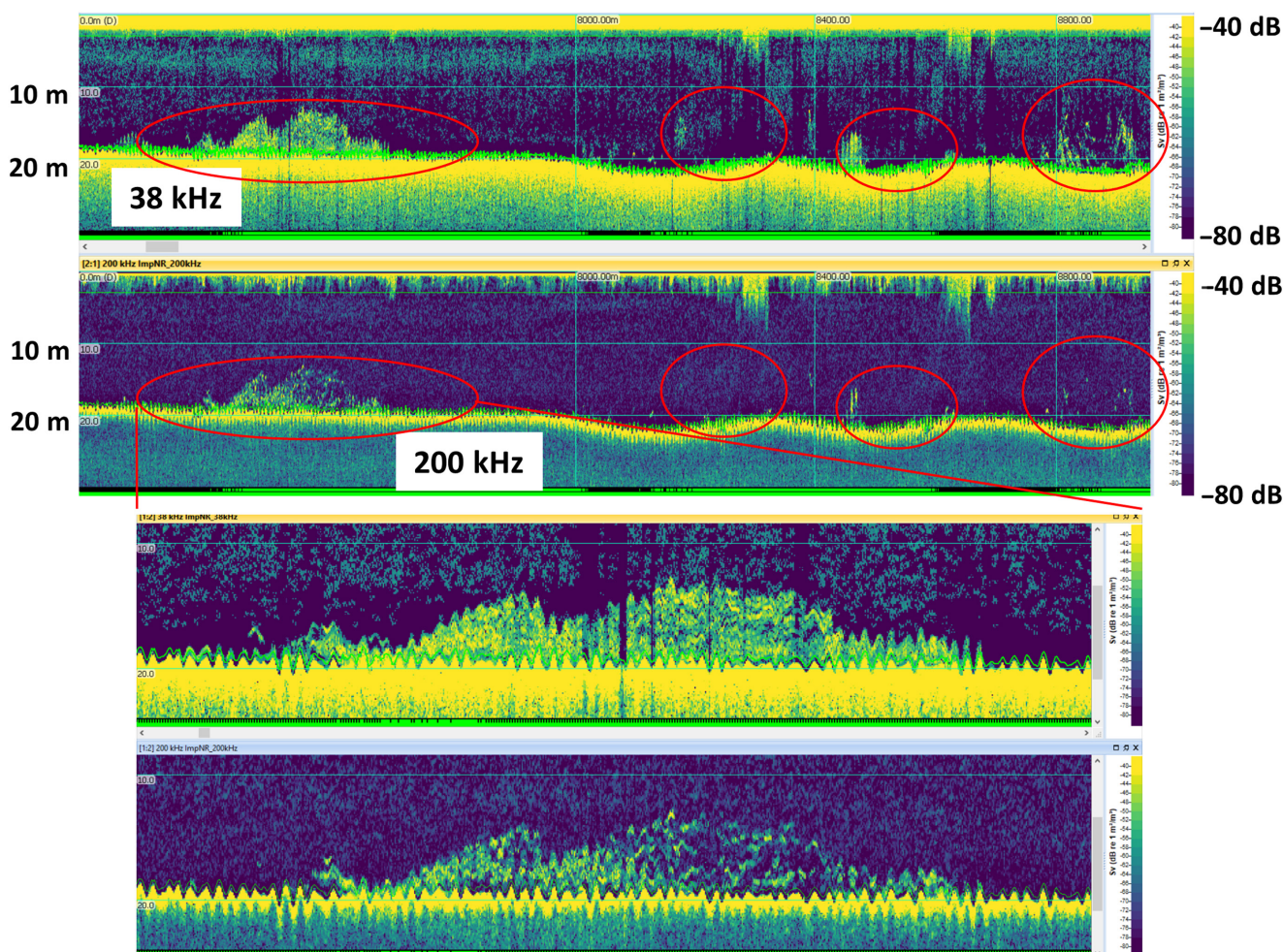**FIGURE 3** The 38-kHz (upper echogram in top panel) and 200-kHz (lower echogram in top panel) echograms from August 11, 2021, showing aggregations of Black Sea Bass (denoted by red boundaries). The lower panel shows an aggregation and the differences in echo patterns between the 38-kHz (upper echogram) and 200-kHz (lower echogram) echograms due to the differences in beam widths between the two acoustic beams.
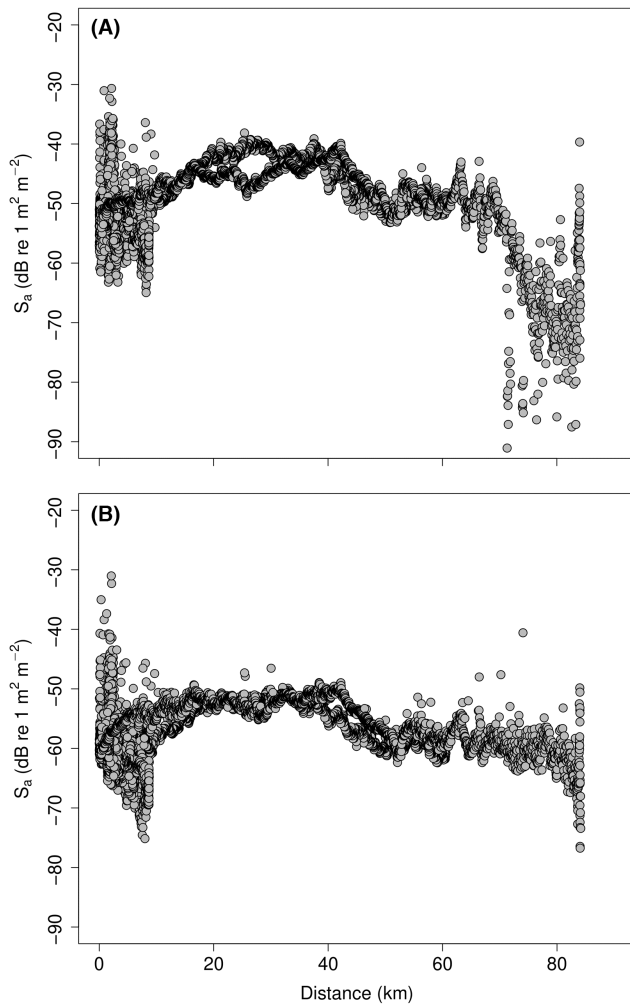
FIGURE 4 Acoustic backscatter (S_a) at (A) 38 kHz and (B) 200 kHz over the duration of the cruise for each 40-m horizontal equivalent distance sampling unit (EDSU). Distance is measured from the geographic midpoint of the Block Island Wind Farm turbines (0 km) to the midpoint of each EDSU.

FIGURE 5 (A) Acoustic water column backscatter ($S_{a,\text{EDSU}}$[38 kHz], where EDSU = equivalent distance sampling unit) and (B) fish backscatter ($S_{a,\text{region}}$[38 kHz]) within 5 km of the geographic midpoint of the Block Island Wind Farm turbines. The vertical dashed lines are the distances between each turbine and the midpoint of the turbines. The distance from the midpoint is 95 m for turbine WTG-3, 835 m for WTG-2 and WTG-4, and 1658 m for WTG-1 and WTG-5.

20–30 km from the BIWF was observed, where the overall level of $S_{a,\text{EDSU}}$(38 kHz) increased by nearly 20 dB and $S_{a,\text{EDSU}}$(200 kHz) increased by about 10 dB (Figure 4). The $S_{a,\text{EDSU}}$(38 kHz) and $S_{a,\text{EDSU}}$(200 kHz) decreased at a 10–20-km range from the BIWF and then increased within 10 km of the BIWF. Within 5 km of the BIWF, $S_{a,\text{EDSU}}$(38 kHz) and $S_{a,\text{region}}$(38 kHz) showed cyclical patterns of increases and decreases (Figure 5). Locations of the peaks in S_a corresponded to the distances between the BIWF geographic midpoint and the location of each turbine, and the increases were nearly 15 dB above the background levels.

Over the course of the 4 days, 462 regions were classified as fish (Table 1). We investigated three different types of distance measures: the distance between each fish region and each turbine, the distance between each region and the geographic midpoint of the BIWF, and the closest
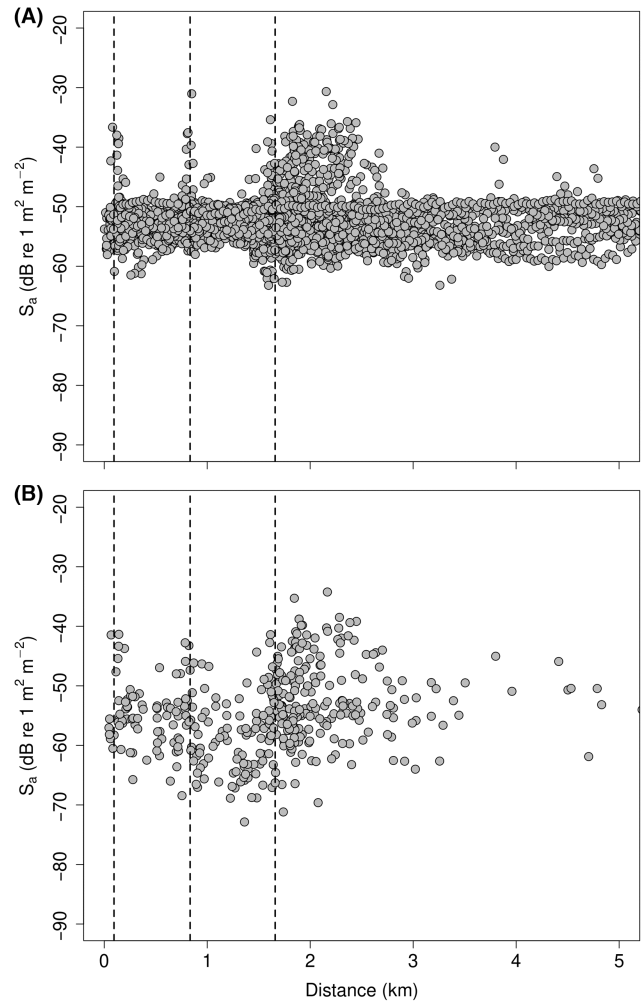
turbine to each region (i.e., the CPA of each region relative to its closest turbine). The mean distance between each region and each turbine ranged from 2.99 to 5.71 km, with WTG-3 having the shortest mean distance and WTG-5 having the longest mean distance. The mean distance of all regions to the geographic midpoint of the BIWF was 2.98 km. The mean CPA distances ranged from 0.55 to 6.62 km; the shortest mean distance was to WTG-2, and the longest mean distance was to WTG-1. The primary reason that the longest mean distance was to WTG-1 is that this turbine was closest to all regions leading to and from the BIWF during transit to/from Woods Hole and to/from anchorage at Block Island. The turbine WTG-5 had 41% of the regions in closest proximity to it, and WTG-2 had the least, as 8% of regions were associated with it (Table 1).

TABLE 1 The number of fish regions and the means (SDs in parentheses) of distances between each region and each turbine, and the number of regions and the means (SDs in parentheses) of distances between each region and its closest turbine (closest point of approach [CPA]). The mean distance between each region and the Block Island Wind Farm geographic midpoint was 2.98 km.

	Each region/turbine		CPA	
Turbine	Number of regions	Mean distance (km)	Number of regions	Mean distance (km)
WTG-1	462	3.75 (5.71)	107	6.62 (11.28)
WTG-2	462	3.29 (5.91)	36	0.55 (0.67)
WTG-3	462	2.99 (6.12)	63	0.62 (0.71)
WTG-4	462	3.02 (6.31)	66	0.60 (0.61)
WTG-5	462	5.71 (6.51)	190	0.61 (0.57)
Total	2310		462	

All turbines had increased acoustic S_a within 0.11–0.24 km of them (Figure 6), and the levels of backscatter were statistically equivalent (pairwise t-test in R) among turbines (Table 2). The distances from each turbine over which the S_a increased from background levels to higher levels were estimated using a polynomial spline ("smooth. spline" function in R, with lambda $= 1 \times 10^{-5}$) fitted to the $S_{a,\text{EDSU}}$(38 kHz) and $S_{a,\text{region}}$(38 kHz) data as a function of CPA distance between the geographic midpoint of each EDSU or region and its closest turbine (WTG$_{\text{CPA}}$). We used the distance to the first local minimum as a measure of the distance at which the turbine acted as an attractive structure, and we defined data that were within this distance as being in close proximity to a turbine (Figure 6). The mean proximity distance was shorter when we used the $S_{a,\text{EDSU}}$ data (0.13 km) than when we used the $S_{a,\text{region}}$ data (0.16 km; Table 2).

Measures of acoustic abundance and vertical distribution for water column backscatter ($S_{a,\text{EDSU}}$[38 kHz]) and fish backscatter ($S_{a,\text{region}}$[38 kHz]) within close proximity (hereafter, "proximate") to each turbine were compared to those measures beyond that distance (hereafter, "remote") using Student's t-test in R (Table 3). Mean proximate water column backscatter was significantly lower than remote water column backscatter by about 0.7 dB, indicating that overall backscatter levels were lower within proximity to turbines. However, fish backscatter was statistically equivalent whether proximate or remote (difference = 0.2 dB), indicating that fish abundance proximate to the turbines was similar to remote fish abundance. The center of mass was approximately 2 m deeper within proximity to turbines for water column backscatter (13 vs. 11 m) and 1 m deeper for fish backscatter (22 vs. 21 m), indicating that fish were distributed closer to the seabed within proximity to the turbines. Inertia was greater within proximity to turbines but was significantly greater only for water column backscatter, indicating that dispersion was similar for fish backscatter whether proximate or remote to turbines,

whereas water column backscatter was more dispersed in proximity to turbines. The aggregation index was lower within proximity to the turbines, indicating that the fish were more loosely distributed near the turbines (i.e., not schooling) than away from the turbines. Interestingly, the measures of equivalent area (the reciprocal of the aggregation index) were not significantly different between proximate and remote regions, indicating that water column backscatter and fish backscatter were evenly distributed whether proximate or remote to turbines. The proportion of the water column occupied was less within proximity to turbines but was significantly less only for water column backscatter, indicating that fish backscatter was equally distributed throughout the water column whether proximate or remote to turbines, while water column backscatter was more concentrated when remote from turbines.

SeapiX data

Single targets were detected in the SeapiX data collected on August 11, 2021, during the spiral patterns around WTG-2–5, and scattering intensity, latitude, longitude, and depth were extracted (WTG-5 data are shown in Figure 7). The distribution of the number of targets surrounding WTG-5 was bimodal, with high numbers at 0.03–0.05 km and 0.19–0.22 km away from the turbine and minimum numbers at 0.13 km (Table 2; Figure 8). The patterns were similar for the other turbines, with minimum numbers first occurring between 0.07 and 0.13 km from the turbine structures (Table 2). The number of targets ramped up and down at the edges of the distribution, possibly because there was no swath overlap on the inside edge of the inside spiral and the outside edge of the furthest outside spiral, but there was overlap in swaths as the vessel spiraled away from the turbines. Bathymetric surveys are designed with swath overlap, but water column surveys with multibeam systems need to account for
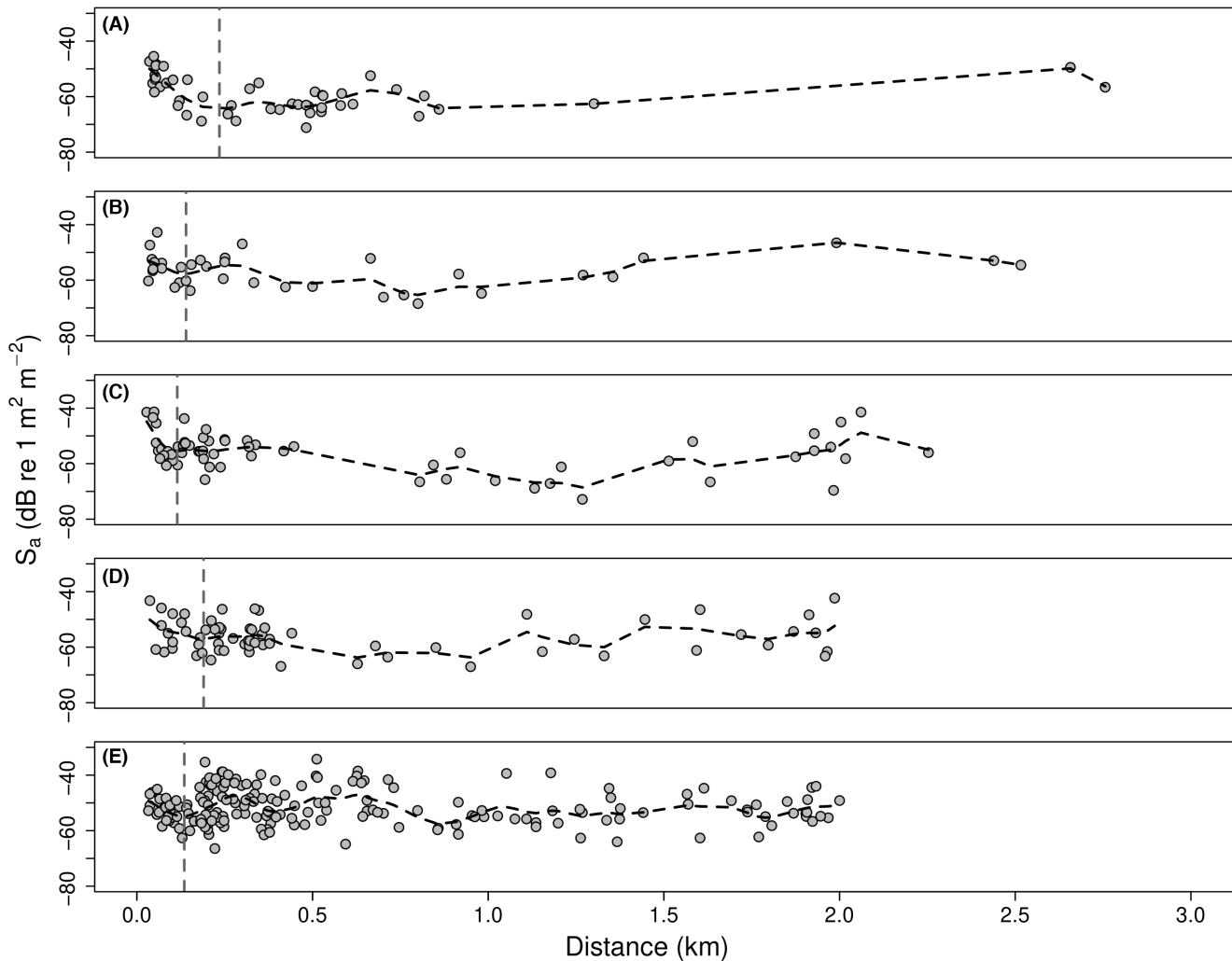
FIGURE 6 Acoustic backscatter (S_a) at 38 kHz for each region classified as fish ($S_{a,region}$). Distance is expressed as the number of kilometers between the midpoint of each region and its closest turbine. Panels (A)–(E) depict turbines WTG-1 to WTG-5, respectively. The vertical dashed line is the location of the first null in the spline (horizontal dashed line), indicating the distance from each turbine where S_a reached a local minimum.

TABLE 2 Distance (km) to the first local minimum (i.e., proximate distance) of a polynomial spline curve applied to the water column backscatter ($S_{a,EDSU}$[38 kHz]), fish backscatter ($S_{a,region}$[38 kHz]), and single targets detected in the SeapiX data, where distance was measured between the geographic midpoint of each equivalent distance sampling unit or region and its closest turbine (WTG$_{CPA}$; CPA is the closest point of approach). Mean $S_{a,region}$(38 kHz) within the proximate distance to each turbine is shown.

Turbine	Distance (km) $S_{a,EDSU}$	Distance (km) $S_{a,region}$	Mean $S_{a,region}$ (dB re 1 m^2 m^{-2})	Distance (km) SeapiX
WTG-1	0.13	0.24	−51.9	
WTG-2	0.14	0.14	−51.2	0.10
WTG-3	0.11	0.12	−47.8	0.08
WTG-4	0.14	0.19	−50.8	0.07
WTG-5	0.13	0.14	−51.0	0.13
Mean	0.13	0.16	−54.1	0.10

swath overlap to minimize potential bias in echo counting and/or echo integration when estimating abundance (Trenkel et al. 2008). Echo strength (peak amplitude of the single-target echo not corrected for the beam pattern) was maximum closest to the turbine, with nearly a 5-dB decrease out to approximately 0.08 km and then an increase out to 0.25 km (Figure 8). The distance at which the minimum echo strength occurred (0.08 km) was closer to WTG-5 than was the distance to the minimum number of targets (0.14 km).

DISCUSSION

We observed a consistent enhanced level of acoustic S_a within 130–160 m of the BIWF turbines, suggesting that the turbines attracted fish out to those distances during our cruise period. We used the distance from a turbine to

TABLE 3 Results of *t*-tests comparing abundance as measured by the total water column backscatter ($S_{a,\text{EDSU}}$[38 kHz]) and fish backscatter ($S_{a,\text{region}}$[38 kHz]), center of mass, inertia, proportion occupied, equivalent area, and aggregation index within the first minimum distance ("proximate"; Table 2) to those beyond the first minimum distance ("remote"). EDSU, equivalent distance sampling unit; $n_{\text{proximate}}$, number of proximate observations; n_{remote}, number of remote observations; $\Delta\mu$, the difference between the means ($\mu_{\text{proximate}} - \mu_{\text{remote}}$); $\mu_{\text{proximate}}$, the mean for each metric for the proximate regions; μ_{remote}, the mean for each metric for the remote regions. Bold *p*-values indicate significance at the 0.05 level.

| Metric	$S_{a,\text{EDSU}}$ or $S_{a,\text{region}}$	$\mu_{\text{proximate}}$	μ_{remote}	$\Delta\mu$	*t*-statistic	*p*-value	$n_{\text{proximate}}$, n_{remote}
S_a (dB re 1 m^2 m^{-2})	$S_{a,\text{EDSU}}$	−51.5	−50.9	−0.685	**−4.42**	**1.11×10^{-5}**	555, 7670
	$S_{a,\text{region}}$	−54.1	−54.3	0.177	0.248	0.805	88, 374
Center of mass (m)	$S_{a,\text{EDSU}}$	13.3	11.4	1.930	**14.2**	**2.83×10^{-40}**	555, 7670
	$S_{a,\text{region}}$	22.1	20.8	1.300	**3.87**	**1.48×10^{-4}**	88, 374
Inertia (m^{-2})	$S_{a,\text{EDSU}}$	24.8	22.5	2.370	**4.18**	**3.29×10^{-5}**	555, 7670
	$S_{a,\text{region}}$	1.13	0.659	0.474	1.90	0.0597	88, 374
Aggregation index (m^{-1})	$S_{a,\text{EDSU}}$	0.028	0.053	−0.024	**−5.13**	**3.06×10^{-7}**	555, 7670
	$S_{a,\text{region}}$	0.214	0.289	−0.076	**−2.59**	**0.0107**	88, 374
Equivalent area (m)	$S_{a,\text{EDSU}}$	124.2	124.0	0.221	0.051	0.9590	555, 7670
	$S_{a,\text{region}}$	19.8	24.0	−4.27	−0.977	0.329	88, 374
Proportion occupied	$S_{a,\text{EDSU}}$	0.323	0.396	−0.073	**−15.1**	**7.36×10^{-46}**	555, 7670
	$S_{a,\text{region}}$	0.231	0.260	−0.029	−1.56	0.121	88, 374
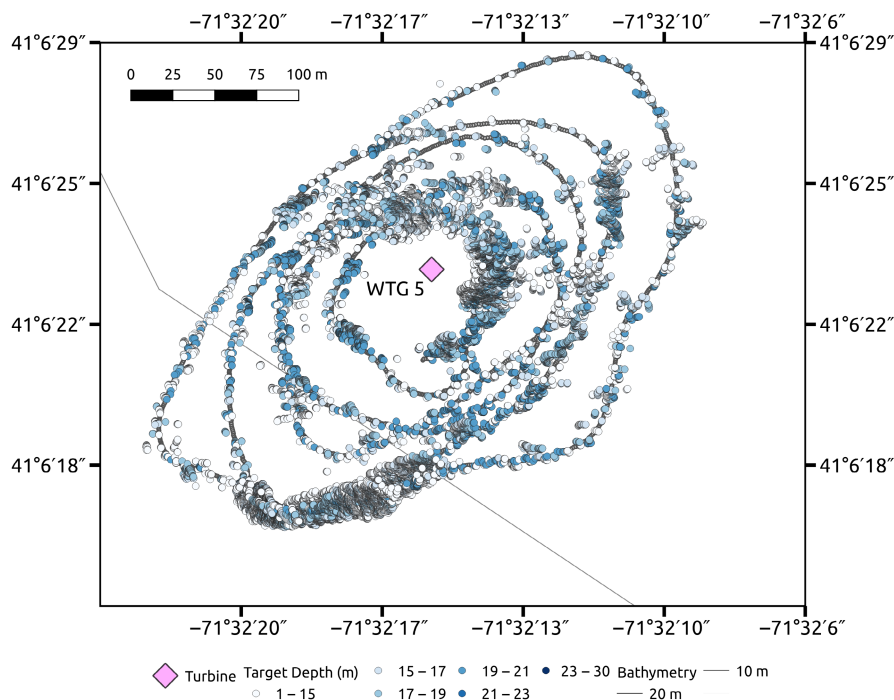
FIGURE 7 Individual targets detected in SeapiX data on August 11, 2021, during a spiral pattern around turbine WTG-5. Symbols are color coded by target depth.

the first local minimum in acoustic S_a (from the single-beam echosounder) or the number of single targets (from the multibeam data) as objective measures of the proximate distance at which the abundance of acoustically detected fish was enhanced. Our distance estimates encompass the distances that have been estimated by other studies using acoustic methods to monitor the spatial distributions of fish and zooplankton around artificial platforms and reefs (typically 50–100 m; e.g., Reynolds et al. 2018; White et al. 2022; Becker et al. 2023). Our closest acoustic measurements using the single-beam echosounder were 28 m from a turbine, so we did not
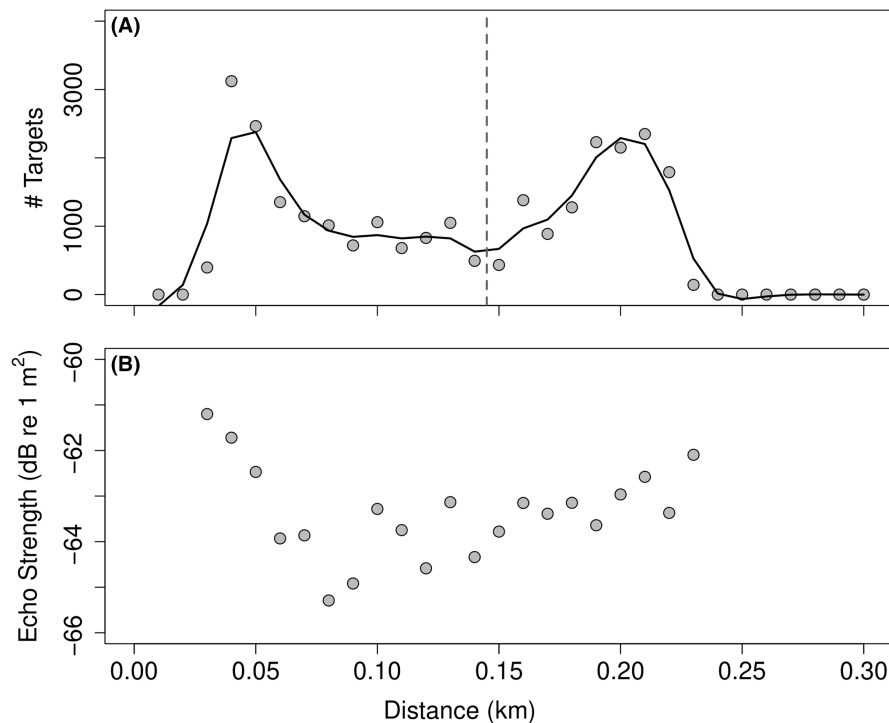
FIGURE 8 (A) Number of targets detected within 10-m range intervals starting from turbine WTG-5 (0 km) outward to 0.30 km. The solid curve is the spline fitted to the data, and the vertical dashed line is the location of the local minimum in the number of targets in relation to WTG-5. (B) Echo strength is presented as a function of distance to WTG-5.

sample within 20–30 m of the turbine structure with the echosounder, which is often considered the zone of direct (i.e., proximate) influence by a reef or platform (Stanley and Wilson 1997; Bergström et al. 2013; van Hal et al. 2017; Becker et al. 2019; Methratta and Dardick 2019). In a downward configuration, the 38-kHz transducer beam width at the deepest part of the survey area (50 m) was 20 m, so we minimized ensonification of any of the turbine structure that could confuse our interpretation of backscatter. However, the conical beam shape limits the proximity to solid objects at which reliable and unbiased acoustic measurements can be made.

Some of the restrictions of sampling close to structure with a single-beam echosounder can be alleviated with multibeam acoustic systems. We collected multibeam data concurrently with the echosounder during the surveys in downward- and side-looking orientations. Advantages to multibeam systems are that they greatly expand the observation swath from 7–20° to 120–150° or greater with high spatial resolution by using beams widths of 1–3°. This allows for better separation of targets that are close to structure and potentially provides the ability to quantify the spatial distribution and abundance of targets that are in close proximity to wind turbines. Two snapshots of the spatial distribution of pelagic targets in relation to a wind turbine are provided in Figure 9. In the traditional

downward orientation (this orientation provides maximal swath along the seabed and is used to map the seabed for bathymetric surveys), the spatial distribution of targets on both sides of the vessel can be monitored simultaneously and the structure can be separated from the pelagic targets. A limitation of this orientation is that the side lobes from the seabed echo can overwhelm the echoes from the pelagic targets (upper panel in Figure 9), thus creating a "dead zone" (e.g., Mayer et al. 2002; Trenkel et al. 2008; Colbo et al. 2014) in the acoustic data. A side-looking orientation can alleviate the issue of the side lobes swamping the water column signal and has the advantage of ensonifying the full water column (lower panel in Figure 9). In this orientation, fish were observed inside the turbine structure. Both of the multibeam orientations demonstrated the ability to visualize targets within meters of the turbine, but processing these data for quantitative purposes is still a research topic.

Although the acoustic data showed an increase in abundance within 160-m proximity to individual turbines, the observed levels close to the turbines did not rise above scattering levels observed at ranges further away. Turbines or other structures are commonly observed to have limited effects on fish distribution at scales of hundreds of meters to kilometers (Bergström et al. 2013; Wilber et al. 2022b). The attraction of natural or artificial structure appears to be limited to close proximity, where fish have refuge from
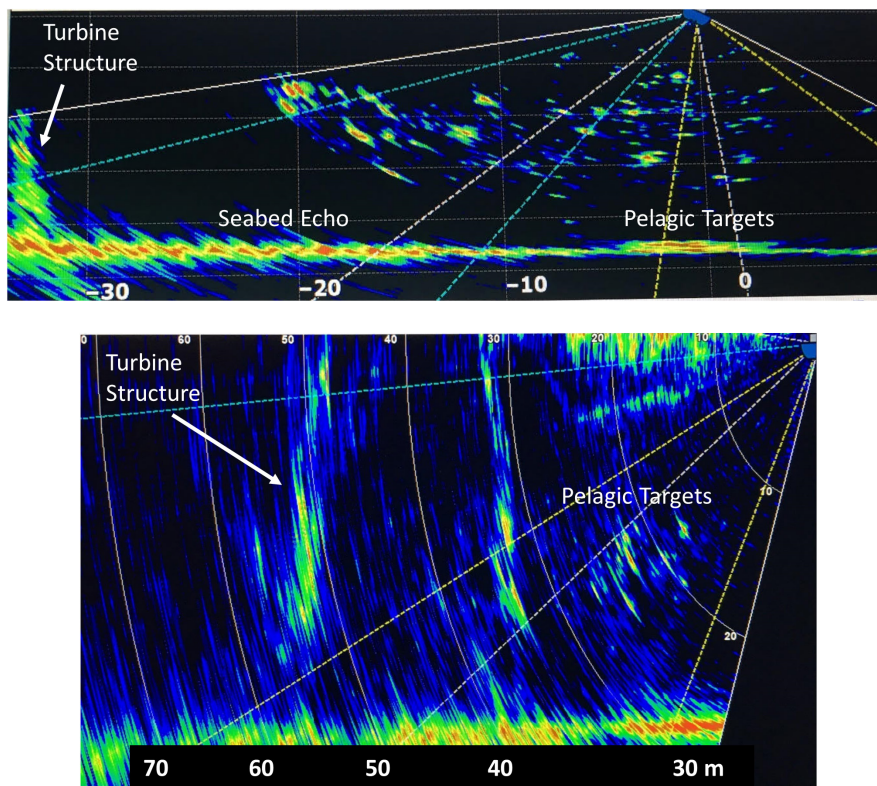
FIGURE 9 Images of pelagic targets collected by the SeapiX multibeam near a Block Island Wind Farm turbine. The top image shows pelagic targets (right side of the image) near a turbine structure with the multibeam in the traditional downward orientation. The blank area between the turbine structure and the targets is due to side lobe suppression. The lower image shows pelagic targets near a turbine with the multibeam in side-looking orientation.

predation and an increased food supply (Bohnsack 1989; Claisse et al. 2014; Bolser et al. 2021). This phenomenon does not appear to be related to the number of turbines, but the size (Stanley and Wilson 1991) or configuration (Reynolds et al. 2018; Becker et al. 2019) of the structures may influence the abundance associated with it. The BIWF has equivalent structures, so it was not possible to discern whether the size or type of structure was an important factor in fish distribution, but the levels of fish backscatter were similar among turbines. This pattern of abundances being similar whether proximate or remote to the BIWF and turbines suggests that the BIWF is not an "oasis in a vast desert," where other topographic features, such as rocky reefs, wrecks, or characteristics of the benthic and pelagic habitat may also attract fish independently of the turbines. Without data prior to construction of the BIWF and given only 4 days of survey data, it is difficult to ascertain the causal mechanisms of our observed spatial patterns and whether they are dependent or independent of the turbines and/or wind farm. These spatial patterns highlight the importance of collecting data at appropriate spatial and temporal scales prior to wind area development.

Hook-and-line catches indicated that the majority of the fish were Black Sea Bass, but we did not use a full suite of angling techniques (e.g., jigging and trolling), gear (e.g., different hook sizes and lures), or bait (e.g., live and frozen), so our catches could be biased toward Black Sea Bass. Skates are unlikely to be acoustically detected because they lie on the seabed and lack a gas-filled swim bladder. Bluefish tend to be near the surface, so they can occupy the near-surface acoustic dead zone (i.e., shallower than the transducer and blanking distance). Scup are well known to be attracted to structure (Wilber et al. 2022b), but it may be that they are inside the structure and therefore difficult to sample using downward-oriented acoustic beams or by angling. Side-looking acoustic systems (multibeam, acoustic lens [adaptive resolution imaging sonar and dual-frequency identification sonar]) and optical systems may be required to sample fauna inside structures (e.g., van Hal et al. 2017). Black Sea Bass aggregate at reefs and structures (Fabrizio et al. 2014; Secor et al. 2021; Wilber et al. 2022b), and they were the largest component of our catch. The aggregations of Black Sea Bass to the south of WTG-5 did not appear to be associated with WTG-5 in the sense that we did not see corridors of fish connecting the fish at WTG-5 and the aggregations. Additionally, the abundance of fish proximate to WTG-5 did not appear to be enhanced by the remote aggregations (the

backscatter at WTG-5 was not greater than at the other turbines), suggesting that the Black Sea Bass were indifferent to the turbine during daylight hours. We unfortunately did not record time with each landed fish to the precision necessary to precisely associate individuals with a particular turbine or distance from turbines, but most of our angling effort was at or near the turbines. Future studies should investigate associations between biological variables (e.g., sex, length, maturity, age, and diet) and offshore wind arrays as well as individual turbines. For example, turbines at the outer edges of wind arrays may have different-sized fish than inner turbines.

Management and conservation of living marine resources constitute a mandate for state and federal fisheries agencies, and evaluating how these resources and ecosystem functions and services may be impacted by OWDAs is an obvious priority. The debate as to whether artificial reefs simply attract biomass of prey or predator species or actually increase production at multiple trophic levels is still active and unresolved (Claisse et al. 2014; Granneman and Steele 2014; Smith et al. 2016; Roa-Ureta et al. 2019; Schwartzbach et al. 2020). With respect to conservation and management, "attraction" results in no net gain or loss of a resource, whereas "production" results in a net gain or loss of that resource. In addition to these population-level effects, offshore wind areas may have effects on ecosystem functions, such as energy flow and food webs (Raoux et al. 2017, 2019; Wang et al. 2019; Halouani et al. 2020), and services (Baulaz et al. 2023). Thus, the roles of OWDAs in "attraction versus production" and ecosystem function are pivotal for developing management strategies and policy as well as sampling strategies that elucidate their role in the continental shelf ecosystem.

From a population assessment perspective, a sampling/monitoring strategy could be to survey an area that encompasses the population of the target species (e.g., the NEFSC bottom trawl survey; Politis et al. 2014) and disregard specific sampling of OWDAs that occur within the population footprint. In this case, any net gain or loss to the population is absorbed into the overall population assessment. Disadvantages to this strategy are that OWDAs could be creating a bias in the spatial and/or temporal distributions, which may or may not be detected by the large-area survey, and there are several mechanisms by which OWDAs could have regional and/or ecosystem implications (Methratta 2021). For example, if OWDAs are acting as attractants, the large-area survey may indicate a population decline, when, in fact, the species distribution is concentrated in OWDAs. If OWDAs increase production, an assumption is that excess biomass spreads (i.e., "spills") out to the broader area. In this case, a large-area survey should detect that increase—unless the increased biomass is attracted to the structures and remains within

OWDAs and the large-area survey indicates no change in biomass. One can argue that biomass "locked" in OWDAs can be considered a separate stock, in which case a separate survey of that stock is required to avert overexploitation of that resource (Pickering and Whitmarsh 1997; Smith et al. 2016; Roa-Ureta et al. 2019). Regardless of whether OWDAs act as fish aggregators, increase production, or both, the most pertinent course for appropriately managing resources that may be impacted by OWDAs seems to be to continue conducting broadscale surveys while adding a program for monitoring OWDAs so that their role can be evaluated in the context of the population as well as incorporated into assessments and ecosystem-based management.

Monitoring of OWDAs will require collecting data over long periods of time at spatial scales of meters (or finer) to kilometers and temporal scales of minutes to years. No single sampling modality can simultaneously achieve these scales, so there must be consideration of different gear, instruments, and platforms. Ideally, "orthogonal" modalities are utilized, where the sampling systems and data are independent of each other. For example, active acoustic systems can be configured to collect data over multiple orders of magnitude in time and space (Trenkel et al. 2011) and are a primary technology that can be used to monitor structures such as turbines (Michaels et al. 2019; Methratta 2021). Single-beam (including split-beam) and multibeam sounders collect data continuously throughout the water column at frequencies commonly between 12 and 500 kHz in narrow (Korneliussen et al. 2009; Weber et al. 2009) and wide (e.g., Demer et al. 2017) bandwidths. When mounted to mobile platforms, such as crewed vessels or autonomous platforms (e.g., Armstrong et al. 2006; Paxton et al. 2019), spatial coverage is typically on the order of tens of square meters to thousands of square kilometers, and temporal coverage is on the order of hours to weeks (i.e., the time required to complete a survey). Sounders that are affixed to stationary moorings (e.g., Horne et al. 2010; Urmy et al. 2012) provide data over temporal scales of seconds to years but only at the location of the mooring. These types of systems are the "bread and butter" of fisheries echosounders and have been commonly used to survey reefs and platforms (Gerlotto et al. 1989; Gledhill et al. 1996; Kang et al. 2011; Holland et al. 2021; Kok et al. 2021).

Acoustic sampling within the boundaries of the turbine/platform and support structure will require submeter resolution so that biological targets can be separated from the solid structure. Acoustic lens technology (van Hal et al. 2017), side-looking multibeam or volumetric sonars, and optical systems (Becker et al. 2019; Bolser et al. 2021) would be ideal for estimating abundance by echo or target

counting within turbine structures and potentially along cables. All of the above systems operate at acoustic frequencies greater than 12 kHz, with most operating above 38 kHz. These systems provide high-quality data out to ranges/depths of about 1 km for the lower frequencies and tens to hundreds of meters for the higher frequencies. To observe much larger areas, we could utilize acoustic systems that operate at lower frequencies. Mid-frequency (3–6 kHz; Lee et al. 2018) and lower (hundreds of hertz to several kilohertz; Makris et al. 2006, 2009, 2019) sonar systems can monitor large areas with a single transmission, effectively providing a snapshot in time of portions of OWDAs or entire OWDAs within seconds. These systems are underutilized in fisheries and plankton acoustics but potentially provide a powerful tool for monitoring OWDAs. The frequencies are in the audible range of many cetacean and marine mammal species (Southall et al. 2019) and fish (Popper and Hawkins 2019), so the duty cycle (i.e., on–off periods) and transmit power levels will need to be considered in order to minimize disturbance to these animals.

A combination of remote technologies (e.g., active and passive acoustics, optics, and environmental DNA) deployed on crewed and autonomous platforms and capture gear will be required to monitor OWDAs at the spatial and temporal scales necessary to understand the roles and impacts of OWDAs on living marine resources. Remote technologies such as acoustics can provide continuous, high-resolution data over multiple orders of magnitude in spatial and temporal scale, but they often lack taxonomic identification to the species level and do not provide biological information. Optical systems provide taxonomic detail but only within meters of the cameras, and artificial light can be problematic by modulating behavior. Mobile capture gear (e.g., bottom and midwater trawls) and fixed gear (e.g., gill nets, fyke nets, longlines, pots, and traps) could be used to collect age, sex, maturity, diet, length, and weight data. These biological data are critical for elucidating the differences between "aggregation" and "production" (Claisse et al. 2014; Smith et al. 2016; Roa-Ureta et al. 2019) as well as for population assessments. Depending on the configuration of turbines and cabling (e.g., fixed or floating turbines), the type(s) of gear that can be deployed may vary among or even within OWDAs (e.g., Ramasco 2021). Our study supports the body of evidence that wind turbines are similar to other artificial structures in that they enhance abundance within 200 m of the structures but seem to have limited effect beyond that. This observation influences decisions on the types of sampling gear, instruments, and platforms that can be used to monitor proximate effects. For example, sampling corridors are proposed as ways to sample and monitor within OWDA boundaries, but these corridors are primarily located midway between turbines. In the case of the BIWF, our acoustic data suggest that sampling midway between turbines would provide no information about the effects of individual turbines. Merging new and historical data streams will require calibrating the new data to existing assessment indices (Miller et al. 2010), which will potentially be made more complicated by changes in sampling methodologies.

CONCLUSIONS

We observed enhanced levels of fish abundance within 200 m of wind turbines at the BIWF during a 4-day survey in August 2021. However, these higher levels were similar to abundances further away (i.e., hundreds to thousands of meters). These observations suggest that the turbines are acting as aggregators at scales of tens of meters but that the effect appears to be limited at broader scales. There was an indication that the turbines influenced (1) vertical distribution, with the acoustic center of mass being deeper within proximity to turbines, and (2) aggregative behavior, with the fish being more loosely distributed within proximity to turbines. Our survey was conducted 5 years after completion of the BIWF, and our results may be indicative of established wind areas, where the fauna may have adapted to the presence of the turbines. However, the BIWF consists of only five turbines, so it may not be large enough to affect broadscale distributions or population-level changes. In addition, other features of the habitat, such as wrecks, rocky reefs, or physical and biological oceanographic attributes that we did not measure, could affect distributions independently of the BIWF.

CONFLICT OF INTEREST STATEMENT
There is no conflict of interest declared in this article.

DATA AVAILABILITY STATEMENT
All data are available upon request to the corresponding author.

ETHICS STATEMENT
Sampling and animal handling protocols were carried out in compliance with the United States National Marine Fisheries Service Institutional Animal Care and Use Policy (NMFS Procedure 04-112-01) and Scientific Research Permit #21002.

REFERENCES

Armstrong, R. A., Singh, H., Torres, J., Nemeth, R. S., Can, A., Roman, C., Eustice, R., Riggs, L., & Garcia-Moliner, G. (2006). Characterizing the deep insular shelf coral reef habitat of the Hind Bank marine conservation district (US Virgin Islands) using the seabed autonomous underwater vehicle. *Continental Shelf Research*, *26*(2), 194–205. https://doi.org/10.1016/j.csr.2005.10.004

Azarovitz, T. R. (1981). A brief historical review of woods hole laboratory trawl survey time series. In W. G. Doubleday & D. Rivard (Eds.), *Bottom trawl surveys* (pp. 62–67, Canadian Special Publication of the Fisheries and Aquatic Sciences 58). Department of Fisheries and Oceans.

Baulaz, Y., Mouchet, M., Niquil, N., & Lasram, F. B. R. (2023). An integrated conceptual model to characterize the effects of offshore wind farms on ecosystem services. *Ecosystem Services*, *60*, Article 101513. https://doi.org/10.1016/j.ecoser.2023.101513

Becker, A., Lowry, M. B., Fowler, A. M., & Taylor, M. D. (2023). Hydroacoustic surveys reveal the distribution of mid-water fish around two artificial reef designs in temperate Australia. *Fisheries Research*, *257*, Article 106509. https://doi.org/10.1016/j.fishres.2022.106509

Becker, A., Smith, J. A., Taylor, M. D., McLeod, J., & Lowry, M. B. (2019). Distribution of pelagic and epi-benthic fish around a multi-module artificial reef-field: Close module spacing supports a connected assemblage. *Fisheries Research*, *209*, 75–85. https://doi.org/10.1016/j.fishres.2018.09.020

Bergström, L., Sundqvist, F., & Bergström, U. (2013). Effects of an offshore wind farm on temporal and spatial patterns in the demersal fish community. *Marine Ecology Progress Series*, *485*, 199–210. https://doi.org/10.3354/meps10344

Bohnsack, J. A. (1989). Are high densities of fishes at artificial reefs the result of habitat limitation or behavioral preference? *Bulletin of Marine Science*, *44*(2), 631–645.

Bohnsack, J. A., & Sutherland, D. L. (1985). Artificial reef research: A review with recommendations for future priorities. *Bulletin of Marine Science*, *37*(1), 11–39.

Bolser, D. G., Egerton, J. P., Grüss, A., & Erisman, B. E. (2021). Optic-acoustic analysis of fish assemblages at petroleum platforms. *Fisheries*, *46*(11), 552–563. https://doi.org/10.1002/fsh.10654

Bull, A. S., & Love, M. S. (2019). Worldwide oil and gas platform decommissioning: A review of practices and reefing options. *Ocean & Coastal Management*, *168*, 274–306. https://doi.org/10.1016/j.ocecoaman.2018.10.024

Bureau of Ocean Energy Management. (2022). Ocean wind 1 offshore wind farm draft environmental impact statement (Vol. 2, OCS EIS/EA BOEM 2022). Bureau of Ocean Energy Management.

Bureau of Ocean Energy Management. (2023). State activities. http://www.boem.gov/renewable-energy/state-activities

Claisse, J. T., Pondella, D. J., 2nd, Love, M., Zahn, L. A., Williams, C. M., Williams, J. P., & Bull, A. S. (2014). Oil platforms off California are among the most productive marine fish habitats globally. *Proceedings of the National Academy of Sciences of the United States of America*, *111*(43), 15462–15467. https://doi.org/10.1073/pnas.1411477111

Clark, S., O'Gorman, J., Despres, L., Silva, V., & Lewis, B. (1999). Research vessel survey data collection and management for northern shrimp (Northeast Fisheries Science Center Reference Document 99-10). National Oceanic and Atmospheric Administration.

Colbo, K., Ross, T., Brown, C., & Weber, T. C. (2014). A review of oceanographic applications of water column data from multi-beam echosounders. *Estuarine, Coastal, and Shelf Science*, *145*, 41–56. https://doi.org/10.1016/j.ecss.2014.04.002

Dainys, J., Gorfine, H., Mateos-González, F., Skov, C., Urbanavičius, R., & Audzijonyte, A. (2022). Angling counts: Harnessing the power of technological advances for recreation fishing surveys. *Fisheries Research*, *254*, Article 106410. https://doi.org/10.1016/j.fishres.2022.106410

Demer, D. A., Andersen, L. N., Bassett, C., Berger, L., Chu, D., Condiotty, J., & Cutter, G. R. (2017). 2016 USA–Norway EK80 workshop report: Evaluation of a wideband echosounder for fisheries and marine ecosystem science (Cooperative Research Report 336). International Council for the Exploration of the Sea.

Fabrizio, M. C., Manderson, J., & Pessutti, J. P. (2014). Home range and seasonal movements of Black Sea Bass (*Centropristis striata*) during their inshore residency at a reef in the Mid-Atlantic Bight. *U.S. National Marine Fisheries Service Fishery Bulletin*, *112*(1), 82–97. https://doi.org/10.7755/FB.112.1.6

Fernandes, P. G., Copland, P., Garcia, R., Nicosevici, T., & Scoulding, B. (2016). Additional evidence for fisheries acoustics: Small cameras and angling gear provide tilt angle distributions and other relevant data for mackerel surveys. *ICES Journal of Marine Science*, *73*(8), 2009–2019. https://doi.org/10.1093/icesjms/fsw091

Foote, K. G., Knudsen, H. P., Vestnes, G., MacLennan, D. N., & Simmonds, E. J. (1987). Calibration of acoustic instruments for fish density estimation: A practical guide (Cooperative Research Report 144). International Council for the Exploration of the Sea.

Frear, P. A. (2002). Hydroacoustic target strength validation using angling creel census data. *Fisheries Management and Ecology*, *9*(6), 343–350. https://doi.org/10.1046/j.1365-2400.2002.00312.x

Gerlotto, F., Bercy, C., & Bordeau, B. (1989). Echo-integration survey around off-shore oil-extraction platforms off Cameroon: Observation of the repulsive effect on fish of some artificially emitted sounds. *Proceedings of the Institute of Acoustics*, *11*(3), 79–88.

Gill, A. B., Degraer, S., Lipsky, A., Mavraki, N., Methratta, E., & Brabant, R. (2020). Setting the context for offshore wind development effects on fish and fisheries. *Oceanography*, *33*(4), 118–127. https://doi.org/10.5670/oceanog.2020.411

Gledhill, C. T., Lyczkowski-Shultz, J., Rademacher, K., Kargard, E., Crist, G., & Grace, M. A. (1996). Ealuation of video and acoustic index methods for assessing reef-fish populations. *ICES Journal of Marine Science*, *53*(2), 483–485. https://doi.org/10.1006/jmsc.1996.0069

Granneman, J. E., & Steele, M. A. (2014). Fish growth, reproduction, and tissue production on artificial reefs relative to natural reefs. *ICES Journal of Marine Science*, *71*(9), 2494–2504. https://doi.org/10.1093/icesjms/fsu082

Halouani, G., Villanueva, C. M., Raoux, A., Dauvin, J. C., Lasram, F. B. R., Foucher, E., Le Loc'h, F., Safi, G., Araignous, E., Robin, J. P., & Niquil, N. (2020). A spatial food web model to investigate potential spillover effects of a fishery closure in an offshore wind farm. *Journal of Marine Systems*, *212*, Article 103434. https://doi.org/10.1016/j.jmarsys.2020.103434

Hare, J. A., Blythe, B. J., Ford, K. H., Godfrey-McKee, S., Hooker, B. R., Jensen, B. M., Lipsky, A., Nachman, C., Pfeiffer, L., Rasser,

M., & Renshaw, K. (2022). NOAA Fisheries and BOEM federal survey mitigation implementation strategy - Northeast U.S. Region (Technical Memorandum NMFS-NE-292). National Oceanic and Atmospheric Administration.

HDR. (2018). Field observations during wind turbine foundation installation at the Block Island Wind Farm, Rhode Island (OCS Study BOPEM 2018-2019). Bureau of Ocean Energy Management.

Holland, M. W., Becker, A., Smith, J. A., Everett, J. D., & Suthers, I. M. (2021). Fine-scale spatial and diel dynamics of zooplanktivorous fish on temperate rocky and artificial reefs. *Marine Ecology Progress Series*, *674*, 221–239. https://doi.org/10.3354/meps13831

Horne, J. K., Urmy, S. S., & Barbee, D. H. (2010). Using sonar to describe temporal patterns of oceanic organisms from the MARS observatory. IEEE. https://doi.org/10.1109/OCEANS.2010.5664614

Jech, J. M., & McQuinn, I. H. (2016). Towards a balanced presentation and objective interpretation of acoustic and trawl survey data, with specific reference to the eastern Scotian Shelf. *Canadian Journal of Fisheries and Aquatic Sciences*, *73*(12), 1914–1921. https://doi.org/10.1139/cjfas-2016-0113

Jech, J. M., & Sullivan, P. J. (2014). Distribution of Atlantic Herring (*Clupea harengus*) in the Gulf of Maine from 1998 to 2012. *Fisheries Research*, *156*, 26–33. https://doi.org/10.1016/j.fishres.2014.04.016

Kang, M., Furusawa, M., & Miyashita, K. (2002). Effective and accurate use of difference in mean volume backscattering strength to identify fish and plankton. *ICES Journal of Marine Science*, *59*(4), 794–804. https://doi.org/10.1006/jmsc.2002.1229

Kang, M., Nakamura, T., & Hamano, A. (2011). A methodology for acoustic and geospatial analysis of diverse artificial-reef datasets. *ICES Journal of Marine Science*, *68*(10), 2210–2221. https://doi.org/10.1093/icesjms/fsr141

Kok, A. C. M., Bruil, L., Berges, B., Sakinan, S., Debusschere, E., Reubens, J., de Haan, D., Norro, A., & Slabbekoorn, H. (2021). An echosounder view on the potential effects of impulsive noise pollution on pelagic fish around windfarms in the North Sea. *Environmental Pollution*, *290*, Article 118063. https://doi.org/10.1016/j.envpol.2021.118063

Korneliussen, R. J. (2018). Acoustic target classification (Cooperative Research Report 344). International Council for the Exploration of the Sea.

Korneliussen, R. J., Heggelund, Y., Eliassen, I. K., Øye, O. K., Knutsen, T., & Dalen, J. (2009). Combining multibeam-sonar and multifrequency-echosounder data: Examples of the analysis and imaging of large euphausiid schools. *ICES Journal of Marine Science*, *66*(6), 991–997. https://doi.org/10.1093/icesjms/fsp092

Lee, W. J., Tang, D., Stanton, T. K., & Thorsos, E. I. (2018). Macroscopic observations of diel fish movements around a shallow water artificial reef using a mid-frequency horizontal-looking sonar. *Journal of the Acoustical Society of America*, *144*, 1424–1434. https://doi.org/10.1121/1.5054013

Makris, N. C., Godø, O. R., Yi, D. H., Macaulay, G. J., Jain, A. D., Cho, B., Gong, Z., Jech, J. M., & Ratilal, P. (2019). Instantaneous areal population density of entire Atlantic Cod and Herring spawning groups and group size distribution relative to total spawning population. *Fish and Fisheries*, *20*(2), 201–213. https://doi.org/10.1111/faf.12331

Makris, N. C., Ratilal, P., Jagannathan, S., Gong, Z., Andrews, M., Bertsatos, I., Godø, O. R., Nero, R. W., & Jech, J. M. (2009). Critical population density triggers rapid formation of vast oceanic fish shoals. *Science*, *323*(5922), 1734–1737. https://doi.org/10.1126/science.1169441

Makris, N. C., Ratilal, P., Symonds, D. T., Jagannathan, S., Lee, S., & Nero, R. W. (2006). Fish population and behavior revealed by instantaneous continental shelf-scale imaging. *Science*, *311*(5761), 660–663. https://doi.org/10.1126/science.1121756

Mayer, L., Li, Y., & Melvin, G. (2002). 3D visualization for pelagic fisheries research and assessment. *ICES Journal of Marine Science*, *59*(1), 216–225. https://doi.org/10.1006/jmsc.2001.1125

Methratta, E. T. (2020). Monitoring fisheries resources at offshore wind farms: BACI vs. BAG designs. *ICES Journal of Marine Science*, *77*(3), 890–900. https://doi.org/10.1093/icesjms/fsaa026

Methratta, E. T. (2021). Distance-based sampling methods for assessing the ecological effects of offshore wind farms: Synthesis and application to fisheries resource studies. *Frontiers in Marine Science*, *8*, Article 674594. https://doi.org/10.3389/fmars.2021.674594

Methratta, E. T., & Dardick, W. R. (2019). Meta-analysis of finfish abundance at offshore wind farms. *Reviews in Fisheries Science & Aquaculture*, *27*(2), 242–260. https://doi.org/10.1080/23308249.2019.1584601

Michaels, W. L., Binder, B., Boswell, K., Chérubin, L. M., Demer, D. A., Jarvis, T., Knudsen, F. R., Lang, C., Paramo, J. E., Sullivan, P. J., & Lillo, S. (2019). Best practices for implementing acoustic technologies to improve reef fish ecosystem surveys: Report from the 2017 GCFI Acoustics Workshop (Technical Memorandum NMFS-F/SPO-192). National Oceanic and Atmospheric Administration.

Miller, T. J., Das, C., Politis, P. J., Miller, A. S., Lucey, S. M., Legault, C. M., Brown, R. W., & Rago, P. J. (2010). Estimation of *Albatross IV* to *Henry B. Bigelow* calibration factors (Northeast Fisheries Science Center Reference Document 10-05). National Oceanic and Atmospheric Administration.

Miller, T. J., Hart, D. R., Hopkins, K., Vine, N. H., Taylor, R., York, A. D., & Gallager, S. M. (2019). Estimation of the capture efficiency and abundance of Atlantic Sea scallops (*Placopecten magellanicus*) from paired photographic–dredge tows using hierarchical models. *Canadian Journal of Fisheries and Aquatic Sciences*, *76*(6), 847–855. https://doi.org/10.1139/cjfas-2018-0024

O'Keefe, C. (2022). Atlantic Sea Scallop Survey Working Group report and recommendations. New England Fishery Management Council.

Paxton, A. B., Taylor, J. C., Peterson, C. H., Fegley, S. R., & Rosman, J. H. (2019). Consistent spatial patterns in multiple trophic levels occur around artificial habitats. *Marine Ecology Progress Series*, *611*, 189–202. https://doi.org/10.3354/meps12865

Pickering, H., & Whitmarsh, D. (1997). Artificial reefs and fisheries exploitation: A review of the 'attraction versus production' debate, the influence of design and its significance for policy. *Fisheries Research*, *31*(1–2), 39–59. https://doi.org/10.1016/S0165-7836(97)00019-2

Politis, P. J., Galbraith, J. K., Kostovick, P., & Brown, R. W. (2014). Northeast fisheries science center bottom trawl survey protocols for the NOAA ship *Henry B. Bigelow* (Northeast Fisheries Science Center Reference Document 14-06). National Oceanic and Atmospheric Administration.

Popper, A., & Hawkins, A. D. (2019). An overview of fish bio-acoustics and the impacts of anthropogenic sounds on fishes. *Journal of Fish Biology*, *94*(5), 692–713. https://doi.org/10.1111/jfb.13948

QGIS. (2022). *QGIS geographic information system*. Open Source Geospatial Foundation Project. https://www.qgis.org/en/site/

Ramasco, V. (2021). Glider study at Hywind Scotland (Report 2021 62861.01). Akvaplan-niva.

Raoux, A., Lassalle, G., Pezy, J. P., Tecchio, S., Safi, G., Ernande, B., Mazé, C., Le Loc'h, F., Lequesne, J., Girardin, V., & Dauvin, J. C. (2019). Measuring sensitivity of two OSPAR indicators for a coastal food web model under offshore wind farm construction. *Ecological Indicators*, *96*(Part 1), 728–738. https://doi.org/10.1016/j.ecolind.2018.07.014

Raoux, A., Tecchio, S., Pezy, J. P., Lassalle, G., Degraer, S., Wilhelmsson, D., Cachera, M., Ernande, B., Le Guen, C., Haraldsson, M., & Grangeré, K. (2017). Benthic and fish aggregation inside an offshore wind farm: Which effects on the trophic web functioning? *Ecological Indicators*, *72*, 33–46. https://doi.org/10.1016/j.ecolind.2016.07.037

R Core Team. (2022). *R: A language and environment for statistical computing*. The R Foundation.

Reynolds, E. M., Cowan, J. H., Jr., Lewis, K. A., & Simonsen, K. A. (2018). Method for estimating relative abundance and species composition around oil and gas platforms in the northern Gulf of Mexico, U.S.A. *Fisheries Research*, *201*, 44–55. https://doi.org/10.1016/j.fishres.2018.01.002

Roa-Ureta, R. H., Santos, M. N., & Leitão, F. (2019). Modelling long-term fisheries data to resolve the attraction versus production dilemma of artificial reefs. *Ecological Modelling*, *407*, Article 108727. https://doi.org/10.1016/j.ecolmodel.2019.108727

Ryan, T. E., Downie, R. A., Kloser, R. J., & Keith, G. (2015). Reducing bias due to noise and attenuation in open-ocean echo integration data. *ICES Journal of Marine Science*, *72*(8), 2482–2493. https://doi.org/10.1093/icesjms/fsv121

Schwartzbach, A., Behrens, J. W., & Svendsen, J. C. (2020). Atlantic cod Gadus morhua save energy on stone reefs: Implications for the attraction versus production debate in relation to reefs. *Marine Ecology Progress Series*, *635*, 81–87. https://doi.org/10.3354/meps13192

Secor, D. H., Bailey, H., Carroll, A., Lyubchich, V., O'Brien, M. H. P., & Wiernicki, C. J. (2021). Diurnal vertical movements in Black Sea Bass (*Centropristis striata*): Endogenous, facultative, or something else? *Ecosphere*, *12*(6), Article e03616. https://doi.org/10.1002/ecs2.3616

Smith, J. A., Lowry, M. B., Champion, C., & Suthers, J. M. (2016). A designed artificial reef is among the most productive marine fish habitats: New metrics to address "production versus attraction". *Marine Biology*, *163*, Article 188. https://doi.org/10.1007/s00227-016-2967-y

Southall, B. L., Finneran, J. J., Reichmuth, C., Nachtigall, P. E., Ketten, D. R., Bowles, A. E., Ellison, W. T., Nowacek, D. P., & Tyack, P. L. (2019). Marine mammal noise exposure criteria: Updated scientific recommendations for residual hearing effects. *Aquatic Mammals*, *45*(2), 125–232. https://doi.org/10.1578/AM.45.2.2019.125

Stanley, D. R., & Wilson, C. A. (1991). Factors affecting the abundance of selected fishes near oil and gas platforms in the northern Gulf of Mexico. *U.S. National Marine Fisheries Service Fishery Bulletin*, *89*(1), 149–159.

Stanley, D. R., & Wilson, C. A. (1997). Seasonal and spatial variation in the abundance and size distribution of fishes associated with a petroleum platform in the northern Gulf of Mexico. *Canadian Journal of Fisheries and Aquatic Sciences*, *54*(5), 1166–1176. https://doi.org/10.1139/cjfas-54-5-1166

Trenkel, V., Ressler, P. H., Jech, M., Giannoulaki, M., & Taylor, C. (2011). Underwater acoustics for ecosystem-based management: State of the science and proposals for ecosystem indicators. *Marine Ecology Progress Series*, *442*, 285–301. https://doi.org/10.3354/meps09425

Trenkel, V. M., Mazauric, V., & Berger, L. (2008). The new fisheries multibeam echosounder ME70: Description and expected contribution to fisheries research. *ICES Journal of Marine Science*, *65*(4), 645–655. https://doi.org/10.1093/icesjms/fsn051

Urmy, S. S., Horne, J. K., & Barbee, D. H. (2012). Measuring the vertical distributional variability of pelagic fauna in Monterey Bay. *ICES Journal of Marine Science*, *69*(2), 184–196. https://doi.org/10.1093/icesjms/fsr205

van Hal, R., Griffioen, A. B., & van Keeken, O. A. (2017). Changes in fish communities on a small spatial scale, an effect of increased habitat complexity by an offshore wind farm. *Marine Environmental Research*, *126*, 26–36. https://doi.org/10.1016/j.marenvres.2017.01.009

Wang, J., Zou, X., Yu, W., Zhang, D., & Wang, T. (2019). Effects of established offshore wind farms on energy flow of coastal ecosystems: A case study of the Rudong offshore wind farms in China. *Ocean and Coastal Management*, *171*, 111–118. https://doi.org/10.1016/j.ocecoaman.2019.01.016

Weber, T. C., Peña, H., & Jech, J. M. (2009). Consecutive acoustic observations of an Atlantic Herring school in the northwest Atlantic. *ICES Journal of Marine Science*, *66*(6), 1270–1277. https://doi.org/10.1093/icesjms/fsp090

White, A. L., Patterson, W. F., III, & Boswell, K. (2022). Distribution of acoustic fish backscatter associated with natural and artificial reefs in the northeastern Gulf of Mexico. *Fisheries Research*, *248*, Article 106199. https://doi.org/10.1016/j.fishres.2021.106199

Wilber, D. H., Brown, L., Griffin, M., DeCelles, G. R., & Carey, D. A. (2022a). Offshore wind farm effects on flounder and gadid dietary habits and condition on the northeastern US coast. *Marine Ecology Progress Series*, *683*, 123–138. https://doi.org/10.3354/meps13957

Wilber, D. H., Brown, L., Griffin, M., DeCelles, G. R., & Carey, D. A. (2022b). Demersal fish and invertebrate catches relative to construction and operation of North America's first offshore wind farm. *ICES Journal of Marine Science*, *79*(4), 1274–1288. https://doi.org/10.1093/icesjms/fsac051

SUPPORTING INFORMATION

Additional supporting information can be found online in the Supporting Information section at the end of this article.